

Non-Markovian Quantal Brownian Motion Model

H. M. Cataldo¹ and E. S. Hernández¹

Received February 20, 1987; revision received August 13, 1987

A non-Markovian version of the quantal Brownian motion model is given. The integrodifferential equations of motion are solved, establishing the analytic form of the resolvent poles and analyzing their properties. An explicit investigation of the poles at zero temperature is performed. In this frame a rule can be found that relates the relevant poles of the non-Markovian resolvent to the eigenvalues of the associated Markovian generator of the motion.

KEY WORDS: Non-Markovian master equation; resolvent poles; zero temperature; non-Markovian/Markovian frequency relation.

1. INTRODUCTION

The determination of the validity of a Markovian description of a relaxation kinetics in either a short-time domain or in physical situations where a neat separation between time scales does not show up is an interesting problem in branches of condensed matter physics. A recent approach to the description of damped collective motion in finite quantal systems such as nuclei, named the quantal Brownian motion (QBM) model, has been recently proposed⁽¹⁾ and a collection of applications have been made⁽²⁻¹¹⁾ that exploit the Markovian limit of the model. Since this is likely not a good approximation for finite systems, we consider it convenient to examine the non-Markovian version of the QBM model and to find a criterion to compare some aspects of the related time evolution and relaxation of the collective mode with those predicted in the Markovian limit.

To this end, in Section 2 we briefly review the characteristics of the QBM model and relate it to alternative descriptions of the decay of har-

¹ Departamento de Física, Facultad de Ciencias Exactas y Naturales, Universidad de Buenos Aires, 1428 Buenos Aires, Argentina.

monic oscillations coupled to a heat bath. We then present the equations of motion in the non-Markovian QBM model, establish the analytic form of the poles of the resolvent of the integral generator of the motion, and analyze the properties of the transition rates upon which these poles depend. An explicit investigation of the characteristics of the poles at zero temperature is presented in Section 3 from a general viewpoint, and a model application is discussed in Section 4. It is shown in Section 5 that from the previous sections one can find a rule that relates the relevant poles of the non-Markovian resolvent to the eigenvalues of the associated Markovian generator of the motion. The major results of this work are summarized in Section 6.

2. THE TRANSITION RATES IN THE NON-MARKOVIAN QBM MODEL

We are interested in the description of the damped motion of a quantal harmonic oscillator immersed in a stationary fermionic reservoir with which it interacts through a standard particle-phonon potential.⁽¹⁻⁵⁾ The system we have in mind is a nucleus where a collective vibration that has been excited, e.g., by photoabsorption or nucleus-nucleus inelastic scattering, undergoes statistical decay, releasing excitation energy to the intrinsic or nucleonic degrees of freedom.⁽¹²⁾ We have recently proposed the QBM model in order to investigate the dynamic and thermodynamic aspects of vibration damping combined with broadening of single-particle (s.p.) lines in nuclear matter,^(1,2,5,7,10) in spherical nuclei,^(3,4) in axially symmetric nuclear matter,^(6,8) and in axially deformed nuclei.^(9,11) Apart from specific details concerning the symmetry of the system, the number and characteristics of the vibration, and the object of a particular investigation, where one may focus either on the collective or on the s.p. dynamics or on both, the essentials of the QBM approach are as follows. One proposes that a Hamiltonian

$$H = \sum_i \hbar \Omega_i \Gamma_i^+ \Gamma_i + H_F + \sum_{\alpha\mu} (\lambda_{\alpha\mu}^{(i)} \Gamma_i^+ b_\mu^+ b_\alpha + \lambda_{\alpha\mu}^{(i)*} \Gamma_i b_\alpha^+ b_\mu) \quad (2.1)$$

generates the evolution of the complete density operator of the system according to the Schrödinger-von Neumann equation of motion. In expression (2.1), we assume that several harmonic modes with frequencies Ω_i and phonon numbers $\Gamma_i^+ \Gamma_i$ may be present, immersed in a fermion heat reservoir with Hamiltonian H_F (whose details are not relevant to the current work), where b_μ^+ and b_μ are the fermion creation and annihilation operators, respectively. The coupling mechanism proceeds according to

fermion excitation (resp. deexcitation) combined with destruction (resp. creation) of a phonon of some class i , with corresponding vertex intensity $\lambda_{\alpha\mu}^{(i)}$. The labels α and μ , respectively, denote s.p. states that can decay into a phonon plus a lower energy s.p. and that can collapse, together with an already existing phonon, into a higher energy fermion.

The reduction procedure applied to the full Schrödinger–von Neumann equation of motion, combined with the neglect of initial correlations and with a weak coupling-like approximation to be explained below, gives rise to a set of equations of irreversible evolution.^(1,2,6–10) The density matrix of each oscillator is driven by a Pauli-like master equation, while the fermionic statistical operator evolves according to a generalized kinetic equation that includes the particle–phonon transition rates, in addition to the two-fermion interaction that may appear in the Hamiltonian H_F .

Far from embarking on a detailed discussion of the QBM model and its various applications, in the present work we wish to investigate the spectral properties of the non-Markovian QBM master equation. This is an important issue in view of the future computations in connection with the nuclear problem, where so far all calculations have been performed in the Markovian limit. On the other hand, the kind of analysis we propose is interesting and useful on purely statistical grounds, since we end up with rules relating the poles of the non-Markovian resolvent to the collision frequencies of the corresponding Markovian limit. For simplicity, we focus on a system consisting of one harmonic oscillation in a Fermi reservoir where the two-body interactions are sufficiently strong with respect to the particle–phonon coupling so that the fermions can be regarded as a thermalized ideal gas within the relaxation scale of the vibration. The non-Markovian master equation for the occupation probability of the n -phonon state then reads

$$\begin{aligned}
 \dot{\rho}_0 &= \frac{2}{\hbar^2} g^2 \int_0^t dt e^{-\gamma\tau} \sum_{\alpha\mu} |\lambda_{\alpha\mu}|^2 \\
 &\quad \times \cos[(\omega_{\alpha\mu} - \Omega)\tau] [\rho_1(t-\tau) \rho_\mu(1-\rho_\alpha) - \rho_0(t-\tau) \rho_\alpha(1-\rho_\mu)] \\
 \dot{\rho}_n &= \frac{2}{\hbar^2} g^2 \int_0^t dt e^{-\gamma\tau} \sum_{\alpha\mu} |\lambda_{\alpha\mu}|^2 \cos[(\omega_{\alpha\mu} - \Omega)\tau] [(\rho_{n+1} - \rho_n)_{t-\tau} \rho_\mu(1-\rho_\alpha) \\
 &\quad + (\rho_{n-1} - \rho_n)_{t-\tau} \rho_\alpha(1-\rho_\mu)]; \quad 1 \leq n \leq N-1 \\
 \dot{\rho}_N &= \frac{2}{\hbar^2} g^2 \int_0^t dt e^{-\gamma\tau} \sum_{\alpha\mu} |\lambda_{\alpha\mu}|^2 \cos[(\omega_{\alpha\mu} - \Omega)\tau] \\
 &\quad \times [-\rho_N(t-\tau) \rho_\mu(1-\rho_\alpha) + \rho_{N-1}(t-\tau) \rho_\alpha(1-\rho_\mu)]
 \end{aligned} \tag{2.2}$$

The symbols in Eq. (2.2) are the same as in previous work⁽¹⁻¹¹⁾ and indicate the following. The oscillator frequency is Ω , while $\omega_{\alpha\mu}$ is the difference $(\varepsilon_\alpha - \varepsilon_\mu)/\hbar$; the quantity g in front of the integral is an overall degeneracy factor related to internal fermion coordinates. N is the maximum allowed number of phonons in the computable oscillator spectrum. The equilibrium density of the fermions is the Fermi distribution at a given temperature T , $\rho_A = [1 + \exp(\varepsilon_A - \varepsilon_F)/T]^{-1}$ for $A = \alpha$ or μ . Notice that the integral in Eqs. (2.2) is a convolution; thus, the diagonal matrix elements of the oscillator density operator appear as evaluated at time $t - \tau$. The parameter γ deserves a special word, since its appearance is related to the current weak coupling approximation. Indeed, one knows from the classical literature regarding the general master equation⁽¹³⁻¹⁸⁾ that the convolution term includes a propagator $U_{cc}(\tau) = \exp[(-i/\hbar) L_{cc}\tau]$, where L_{cc} is the Liouvillian in correlation space, namely the one generating the evolution of the system between two interaction vertices. Our version of the master equation in the QBM model contains the approximation

$$U_{cc}(\tau) \approx \exp[(-i/\hbar)(L_F + L_{\text{oscillator}})\tau - \gamma\tau] \quad (2.3)$$

In fact, the above assumption does not fit the usual weak coupling limit,⁽¹⁹⁾ since in this model we are assuming that some part of the total interaction involves unobserved or disregarded channels whose overall manifestation is an inelastic particle-phonon collision, this inelasticity being proportional to the correlation width or energy spread γ .

It is worthwhile noticing at this point that the Markovian limit of the master equation (2.2) presents non-Gibbsian equilibrium behavior.⁽²⁰⁾ Indeed, we may write the equilibrium solution of the Markovian master equation⁽¹⁾ for any temperature as

$$\rho_n^{(0)} = \frac{1}{Z} \left(\frac{W_-}{W_+} \right)^n \quad (2.4)$$

where Z is the normalizing factor or partition function. Now, the ratio W_-/W_+ coincides with the canonical Boltzmann weight $\exp(-\hbar\Omega/T)$ if and only if $\gamma = 0$, i.e., if the dissipative mechanism proceeds through strictly elastic collisions. We could, however, regard expression (2.4) as a definition of an "effective" temperature

$$T_{\text{eff}}(T, \gamma) = -\frac{\hbar\Omega}{\ln(W_-/W_+)} \quad (2.5)$$

In other words, the stationary state of the Brownian oscillator that undergoes inelastic collisions with fermions in a heat bath depends on both

parameters of energy spread, a macroscopic and a microscopic one, respectively, the temperature T and the correlation width γ . This is related to the fact that the inelasticity spread γ represents unobserved interaction channels, which, however, participate in the overall equilibration process; the effective temperature (2.5) is then the thermodynamic force that describes equilibrium among all degrees of freedom, including the disregarded ones. This non-Gibbsian behavior has been observed by other authors^(21,22) who consider a harmonic oscillator strongly coupled to a bath of harmonic oscillators.

In order to solve the integrodifferential equations (2.2), we algebraize them, introducing the Laplace transforms $\rho_n(s)$ for each occupation number, obtaining

$$\begin{aligned}
 s\rho_0(s) - \rho_0(t=0) &= W_+(s)\rho_1(s) - W_-(s)\rho_0(s) \\
 s\rho_n(s) - \rho_n(t=0) &= W_+(s)[\rho_{n+1}(s) - \rho_n(s)] \\
 &\quad + W_-(s)[\rho_{n-1}(s) - \rho_n(s)], \quad 1 \leq n \leq N-1 \\
 s\rho_N(s) - \rho_N(t=0) &= -W_+(s)\rho_N(s) + W_-(s)\rho_{N-1}(s)
 \end{aligned} \tag{2.6}$$

with the microscopic transition rates

$$W_{\pm}(s) = \frac{2g^2}{\hbar^2} \sum_{\alpha\mu} |\lambda_{\alpha\mu}|^2 \frac{s + \gamma}{(s + \gamma)^2 + (\omega_{\alpha\mu} - \Omega)^2} \rho_{\{\mu\}}(1 - \rho_{\{\alpha\}}) \tag{2.7}$$

In this frequency representation the inhomogeneous linear system is simply

$$\rho(s) = R(s)\rho(t=0) \tag{2.8}$$

for the vector ρ with components ρ_n in either the time (t) or the frequency (s) representation, with the resolvent

$$R(s) = \frac{1}{s - M(s)} \tag{2.9}$$

where $M(s)$ is the tridiagonal matrix appearing on the rhs of Eq. (2.6). If $s=0$, the matrix $M(0)$ is the generator of the motion in the standard (Markovian) QBM model⁽¹⁾ with inelastic collisions.⁽²⁾ As we anti-transform equation (2.8), we obtain the desired time evolution as

$$\rho(t) = \sum_{s_r = M(s_r)} \text{Res}[R(s), s_r] e^{s_r t} \rho(0) \tag{2.10}$$

where the amplitudes of each decaying exponential are the residues at the poles s_r of the resolvent $R(s)$. The evaluation of the poles reduces to the spectral problem of a generator $M(s)$, whose solution has been presented in previous QBM work and reads

$$s_r = -W_+(s_r) - W_-(s_r) + 2[W_+(s_r)W_-(s_r)]^{1/2} \cos \frac{r\pi}{N+1} \quad (2.11)$$

$$s_{N+1} = 0$$

with $r = 1, \dots, N$.

From Eq. (2.11) it turns out that a couple of simpler problems may be formulated; indeed, if we assume that the ratio $T/\hbar\Omega$ is low enough that we can neglect the probability of populating oscillator states with more than one quantum, we are left with just two poles, namely

$$s_1 = -[W_+(s_1) + W_-(s_1)], \quad s_2 = 0 \quad (2.12)$$

On the other hand, at absolute zero the “upward-going” transition rate $W_-(s)$ generally vanishes, since fermion labels α, μ correspond to particles and holes ($\rho_\alpha = 1 - \rho_\mu = 0$). Then, in such a case, the poles are

$$s_1 = -W_+(s_1), \quad s_2 = 0 \quad (2.13)$$

In later sections we will concentrate in the latter problem as stated in Eq. (2.13). However, before attempting the detailed computation of the s_1 poles, we would like to establish the most general appearance of the transition rates $W_\pm(s)$ at arbitrary temperatures. Such a study is especially interesting if we consider an infinite, translationally invariant fermion environment with s.p. states characterized by momenta $\mathbf{k}_\alpha, \mathbf{k}_\mu$ and where the oscillator represents an acoustic-like collective mode with momentum \mathbf{q} .⁽¹⁾ We further assume that the collision vertex is momentum-conserving, so that $\mathbf{k}_\alpha = \mathbf{k}_\mu + \mathbf{q}$. Under such conditions, and adopting polar coordinates (r, φ, z) in \mathbf{k}_μ space, we find for the transition rates, after some calculations (see the Appendix),

$$W_\pm(s) = g^2 \frac{|\lambda|^2}{\hbar^2} L^3 \int_{-q/2}^{\infty} dz \frac{s + \gamma}{(s + \gamma)^2 + [\epsilon(z)/\hbar]^2} R_\pm(z) \quad (2.14)$$

In order to derive Eq. (2.14) we supposed that the coupling matrix elements are essentially identical to a single parameter λ if as the z component of the momentum is higher than $-q/2$ and zero otherwise. This is a rule that forbids, at zero temperature, interaction events that would annihilate a phonon transferring a particle from one to another level below

the Fermi sea (cf. Fig. 1 in Section 3). The volume of the box, L^3 , appears in the continuum limit of the summation over momentum states and the radial integrals $R_{\pm}(z)$ can be cast as⁽²³⁾

$$R_+(z) = \frac{1}{1 - \exp\{-[\varepsilon(z) + \hbar\Omega]/T\}} k_T^2 \times \ln \left[\frac{1 + \exp[-(z^2 - F^2)/k_T^2]}{1 + \exp\{-[(z + q)^2 - F^2]/k_T^2\}} \right] \tag{2.15a}$$

$$R_-(z) = (\exp\{[z^2 - (z + q)^2]/k_T^2\}) R_+(z) \tag{2.15b}$$

In Eqs. (2.15), F denotes the Fermi momentum, while k_T is the thermal momentum $(2mT)^{1/2}/\hbar$. The energy variable in the denominator of the Breit–Wigner filter can be written as

$$\begin{aligned} \varepsilon(z) &= \frac{\hbar^2 q^2}{2m} + \hbar q \left(\frac{\hbar z}{m} - c_s \right) \\ &= \frac{\hbar^2 q}{m} (z - z_0) \end{aligned} \tag{2.16}$$

where we have introduced the acoustic dispersion law $\Omega = c_s |\mathbf{q}|$ and momentum conservation into the difference $\varepsilon_\alpha - \varepsilon_\mu - \hbar\Omega$. We can then realize from Eq. (2.15b) that the radial integral $R_-(z)$ vanishes as T vanishes, as already set when writing expressions (2.13). Notice, however, that as T approaches zero, one has to be careful with the limits in expression (2.15a), since different regions of momentum space contribute differently according to the relative location of z and $z + q$ with respect to the Fermi momentum. This situation is dealt with in Section 3.

For finite temperatures T , the transition rates in (2.14) must be computed numerically. It is interesting and useful for future discussion to perform a dimensional analysis of expression (2.14) and exhibit some relevant size parameters. Such an analysis is not unique and in what follows we just display one of the various possibilities. We first notice that the Breit–Wigner kernel in (2.14) can be expressed as a distribution in momentum space,

$$F(z, s) = v_q \frac{s + \gamma}{(s + \gamma)^2 + [\varepsilon(z)/\hbar]^2} = \frac{\eta}{\eta^2 + (z - z_0)^2} \tag{2.17}$$

with a momentum variable

$$\eta = (s + \gamma)/v_q \tag{2.18}$$

where $v_q = \hbar q/m$ is a velocity related to the phonon momentum. The transition rates thus read

$$W_{\pm}(s) \equiv W_{\pm}(\eta) = \omega_{\lambda}^2 \frac{L^3}{v_q} \int_{-q/2}^{\infty} dz F(z, s) R_{\pm}(z) \quad (2.19)$$

with $\omega_{\lambda} = g\lambda/h$ setting a characteristic frequency associated with the interaction strength and the number of internal degrees of freedom per particle. We now observe that the integral in (2.19) possesses the dimension of a square momentum $\langle k^2(s) \rangle_{\pm}$. A dimensional analysis then allows us to write the transition rate as

$$W_{\pm}(s) = \omega_{\lambda} r_{\text{eff}}^2 \langle k^2(s) \rangle_{\pm} \quad (2.20)$$

where

$$r_{\text{eff}} = \left(\frac{1}{2\pi} \frac{g\lambda mL^3}{\hbar^2 q} \right)^{1/2} \quad (2.21)$$

plays the role of an effective interaction range. In fact, apart from a dimensionless factor relating energy parameters of the system, r_{eff} is the geometric average between the size of the box and the phonon wavelength q^{-1} . We can then anticipate that the location of the poles [cf. Eq. (2.11)] is strongly dependent on the competition between the effective length and the rms momentum $[\langle k^2(s) \rangle]^{1/2}$. We return to this point in Sections 3 and 4.

3. THE RESOLVENT POLES AT ZERO TEMPERATURE

The problem outlined in Section 2 essentially reduces to solving Eq. (2.11) under particular conditions in order to locate the characteristic decay frequencies of the vibrator. In this section we will concentrate on the $T=0$ case, where the secular equation is given by (2.13). Before embarking on the computation of the transition rate $W_{+}(s_1)$, we analyze the general properties of the expected oscillator density vector as a function of time. In this case it is a straightforward algebraic exercise to find the resolvent matrix, since it is just the inverse of

$$s - M(s) = \begin{bmatrix} s & -W & 0 & 0 & \dots & 0 \\ 0 & s+W & -W & 0 & \dots & 0 \\ 0 & 0 & s+W & -W & & \vdots \\ \vdots & \vdots & & & \ddots & 0 \\ \vdots & \vdots & & & & -W \\ 0 & 0 & \dots & & & s+W \end{bmatrix} \quad (3.1)$$

where $W = W_+(s)$. The resolvent can be seen to be

$$R(s) = \begin{bmatrix} \frac{1}{s} & \frac{W}{s(s+W)} & \frac{W^2}{s(s+W)^2} & \frac{W^3}{s(s+W)^3} & \cdots & \frac{W^N}{s(s+W)^N} \\ 0 & \frac{1}{s+W} & \frac{W}{(s+W)^2} & \frac{W^2}{(s+W)^3} & \cdots & \frac{W^{N-1}}{(s+W)^N} \\ 0 & 0 & \frac{1}{s+W} & \frac{W}{(s+W)^2} & \cdots & \frac{W^{N-2}}{(s+W)^{N-1}} \\ \vdots & \vdots & \vdots & \ddots & \ddots & \vdots \\ 0 & 0 & 0 & \cdots & 0 & \frac{1}{s+W} \end{bmatrix} \tag{3.2}$$

In order to fix ideas without losing generality, we select a particular initial condition, $\rho_n(0) = \delta_{n,1}$. Different choices represent extension exercises that can be easily undertaken. Thus, the Laplace transform of the density vector is

$$\begin{aligned} \rho_0(s) &= W/(s+W)s \\ \rho_1(s) &= 1/(s+W) \\ \rho_n(s) &= 0 \quad (n \geq 2) \end{aligned} \tag{3.3}$$

It will be shown below that for the system under consideration the poles are single (except for a null measure set in parameter space). Consequently, the amplitudes governing the evolution of the element $\rho_0(t)$ are

$$A(0) = \lim_{s \rightarrow 0} \frac{W_+(s)}{s + W_+(s)} = 1 \tag{3.4}$$

and

$$\begin{aligned} A(s_1) &= \frac{W_+(s)}{s_1} \lim_{s \rightarrow s_1} \frac{s - s_1}{s + W_+(s)} \\ &= - \lim_{s \rightarrow s_1} \frac{s - s_1}{s + W_+(s)} \end{aligned} \tag{3.5}$$

The inverse transform of Eqs. (3.3) is then

$$\begin{aligned}\rho_0(t) &= 1 + \sum_{s_1} A(s_1) e^{s_1 t} \\ \rho_1(t) &= - \sum_{s_1} A(s_1) e^{s_1 t} \\ \rho_n(t) &= 0 \quad (n \geq 2)\end{aligned}\tag{3.6}$$

where the summation indicates that the pole equation $s_1 = -W_+(s_1)$ may possess more than one solution; if that happens, the initial condition demands that

$$\sum_{s_1} A(s_1) = -1\tag{3.7}$$

Let us now take a look at the transition rate $W_+(s)$ in Eq. (2.7). We notice that for zero temperature, the restriction for states α and μ to lie above and below the Fermi level, together with the linear momentum conservation law, determines the shape of the integration domain. The integration to be carried out is

$$W_+(s) = \frac{2g^2}{\hbar^2} |\lambda|^2 L^3 \int dz \int r dr \frac{s + \gamma}{(s + \gamma)^2 + [\varepsilon(z)/\hbar]^2}\tag{3.8}$$

while the integration domain is the half-croissant-like region depicted in Fig. 1. The result of this calculation is

$$W_+(s) \equiv W_+(\eta) = \omega_\lambda r_{\text{eff}}^2 \langle k^2(\eta) \rangle\tag{3.9}$$

with

$$\begin{aligned}\langle k^2(\eta) \rangle &= \eta \left\{ -q[1 + \ln(\eta^2 + k_s^2)] + z_\alpha \ln[\eta^2 + (F - z_\alpha)^2] \right. \\ &\quad - z_\mu \ln[\eta^2 + (F - z_\mu)^2] + \frac{(\eta^2 + F^2 - z_\mu^2)}{\eta} \text{tg}^{-1} \left(\frac{F - z_\mu}{\eta} \right) \\ &\quad \left. - \frac{(\eta^2 + F^2 - z_\alpha^2)}{\eta} \text{tg}^{-1} \left(\frac{F - z_\alpha}{\eta} \right) + \frac{2k_s q}{\eta} \text{tg}^{-1} \left(\frac{k_s}{\eta} \right) \right\}\end{aligned}\tag{3.10}$$

where

$$k_s = mc_s/\hbar\tag{3.11a}$$

$$z_\mu = k_s - q/2\tag{3.11b}$$

$$z_\alpha = k_s + q/2\tag{3.11c}$$

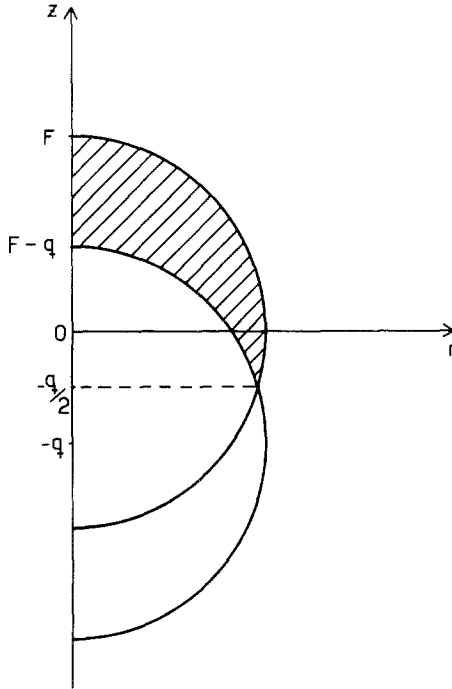


Fig. 1. The domain of integration of the transition probability in the (k_z, k_r) plane is denoted by the shaded area.

Actual evaluation of the poles should correspond to specific problems, since there are too many parameters involved to extract any relevant conclusion from a general analysis. Indeed, so far we have not specified the sizes of the interaction strength λ , the sound velocity c_s , the phonon energy $\hbar\Omega$ (or, equivalently, the phonon momentum q), the size L of the box, and the Fermi momentum, or density, of the particles. We present a particular illustration in the next section.

4. THE BEHAVIOR OF THE POLES IN A MODEL APPLICATION

In this section we specialize to a set of parameters adequate to a specific system and analyze the characteristic of the poles and the time evolution of the oscillator density in the current non-Markovian approach. As stated at the beginning of Section 2, the problem we have in mind concerns the decay of a quantized collective vibration of the “fluid” in the interior of a heavy nucleus due to phonon–nucleon coupling and is of

interest as a paradigm of non-Markovian behavior, since the macroscopic and microscopic scales in the nuclear domain are rather similar and a kinetic description without memory should, in principle, not be allowed. We then fix the parameters as follows:

$$\text{Fermi momentum } F = 1.38 \text{ fm}^{-1}$$

$$\text{phonon energy } \hbar\Omega = 13 \text{ MeV}$$

$$\text{inelasticity spread } \hbar\gamma = 100 \text{ MeV}$$

$$\text{sound speed } c_s = 75 \times 10^{21} \text{ fm/sec}$$

$$\text{spin-isospin degeneracy } g = 4$$

We assume that the poles s are complex with negative real part, i.e.,

$$s_1 = -v + ib \quad (4.1)$$

and look for the real, dimensionless solutions,

$$v/\gamma = (W_+/\gamma)(v/\gamma) \quad (4.2)$$

in a graphical fashion. The situation is depicted in Fig. 2, where we have plotted the rate $W(v/\gamma)/\gamma$ as a function of v/γ for different values of the parameter $\omega_\lambda r_{\text{eff}}^2$, which contains both the interaction strength and the box size. The solutions of Eq. (4.2) are then the intersections with the bisectrix.

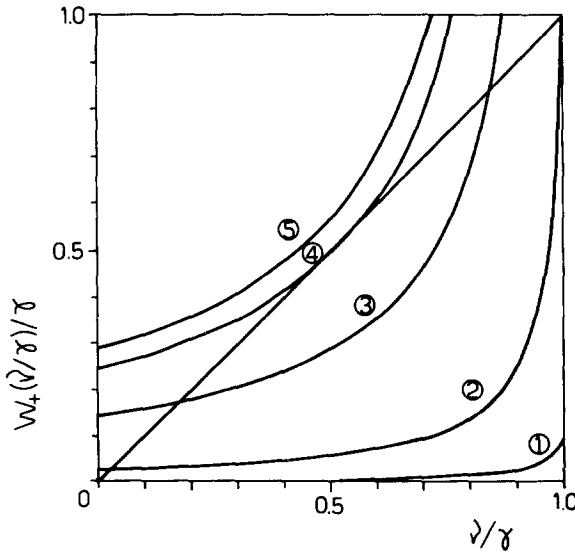


Fig. 2. Graphical solution of the equation defining the singularities of the resolvent. The values of $\omega_\lambda r_{\text{eff}}^2$ for the curves 1–5 are, respectively (in $10^{21} \text{ sec}^{-1} \text{ fm}^2$), 8.290, 82.90, 414.5, 715.3, and 829.0.

It is clear from inspection of this plot that three different regimes show up, namely (1) one low decay frequency located near the origin, while $W_+(1)/\gamma$ remains below unity; (2) one low and one high frequency, the latter departing from the value $v_< = \gamma$ toward smaller values as $\omega_\lambda r_{\text{eff}}^2$ increases; this regime lasts until the two poles merge into a single one at $v_> = v_< = \gamma/2$ and this condition occurs when $W_+(1/2)/\gamma$ equals unity; (3) for higher parameter values, no real pole occurs.

Let us now investigate the characteristic of each regime and of the transitions from one into the other. On the one hand, we locate a first transition at $W_+(1)/\gamma = 1$; regime 1 (resp. regime 2) corresponds to $W_+(1)/\gamma < 1$ [resp. $W_+(1)/\gamma > 1$]. The ratio $W_+(1)/\gamma$ can be expressed as follows. If we compute the square momentum in (3.10) for $\eta = 0$, we get

$$\langle k^2(0) \rangle = 2\pi k_s q \tag{4.3}$$

Using (3.11a) and the acoustic dispersion law, we realize that this quantity is just the inverse of the zero-point dispersion of the oscillator,

$$\langle k^2(0) \rangle = \pi 2m\Omega/\hbar = \pi/\sigma^2 \tag{4.4}$$

and consequently, for $v/\gamma = 1$,

$$W_+(1)/\gamma = \pi\omega_\lambda r_{\text{eff}}^2/\gamma\sigma^2 \tag{4.5}$$

We can now attempt an interpretation of the single-real-pole regime 1. Equation (4.5) tells us that if $\pi\omega_\lambda r_{\text{eff}}^2 \ll \sigma^2\gamma$, we typically get curve 1 in Fig. 2. In this case, we are either in a very weak coupling regime ($\omega_\lambda \ll \gamma$), or within a rather small box ($L \ll \sigma$) or have a combination of conditions. The combined effect can be visualized as depicted in Fig. 3a; the zero-point spread of the vibration is large enough for the oscillator to “see” a highly localized box. In other words, the probability clouds of the oscillator ground state and first few excited states almost fill the box uniformly. We notice that this geometrical viewpoint implies a separation between length scales that is typical of a Markovian description: the interaction domain (the box) is much smaller than a length parameter associated with the collective motion. We feel it is safe to assert that the Markovian approximation to the non-Markovian evolution ought to be adequate within this range of parameters.

As $\omega_\lambda r_{\text{eff}}^2$ increases, the above distinction between length scales becomes fuzzier (the “size” of the zero-point vibration approaches that of the interaction domain). We can observe in Fig. 2 the evolution of the low-frequency poles along the line $f(v/\gamma) = v/\gamma$. The transition between the single-pole to the double-pole regime takes place when $\omega_\lambda r_{\text{eff}}^2 = \gamma\sigma^2/\pi$ [cf. Eq. (4.5)] and according to the above line of reasoning, we can draw a



Fig. 3. Schematic comparison between the size of the effective fermion configuration space and the oscillator spread for (a) very weak interaction (curve 1 in Fig. 2, see text for description) and (b) moderately weak interaction (curve 3 in Fig. 2).

picture like that of Fig. 3b to represent this second regime. In fact, we may now imagine that the interaction domain contains more structure of the oscillator wave functions. According to the neighborhood where a particle-oscillator collision takes place, such an event could involve the wave packet components that contribute to the peak or the more incoherent ones giving rise to the tails. The former events resemble, or keep the track, of the Markovian-like process in the first regime and may thus occur at the low-frequency rate, while the high-frequency pole should be rather related to the coupling among the particles and the less coherent components of the oscillator wave functions. It is then clear that this distinction becomes meaningless as the interaction parameter increases, since these wave functions become more and more localized within the coupling range; consequently, the two poles approach each other along the bisecting line. It is also evident that this regime may persist until both poles collapse together at $v/\gamma = 1/2$. From this stage on, further increase of the parameter $\omega_\lambda r_{\text{eff}}^2$ leads to regime 3, where no real solution to our spectral problem can be found.

We can easily understand this effect as follows: a glance at Eq. (2.7) and a bit of algebra quickly tell us that the quantity $|\omega_{\alpha\mu} - \Omega|$ is bounded, due to linear momentum conservation, by the rule

$$\sup |(\omega_{\alpha\mu} - \Omega)| = \Omega \quad (4.6)$$

If we assume (i) $\gamma \gg \Omega$ and (ii) $|\gamma + s| \gg \Omega$, we extract, from (2.7), the approximation

$$W_+(s) \approx \frac{2g^2}{\hbar^2} \sum_{\alpha\mu} \frac{|\lambda_{\alpha\mu}|^2}{\gamma + s} \quad (4.7)$$

A large sequence of numerical trials demonstrates that (4.7) holds for γ , $|\gamma + s| \geq 10\Omega$. Then, the poles are the roots of

$$s(\gamma + s) = -2 \sum_{\alpha\mu} |\lambda'_{\alpha\mu}|^2 \tag{4.8}$$

with $\lambda'_{\alpha\mu} = g\lambda_{\alpha\mu}/\hbar$

$$s = -\frac{1}{2}\gamma \left\{ 1 \pm \left[1 - (8/\gamma^2) \sum_{\alpha\mu} |\lambda'_{\alpha\mu}|^2 \right]^{1/2} \right\} \tag{4.9}$$

We then see that if

$$g^2 \sum_{\alpha\mu} |\lambda_{\alpha\mu}|^2 > \frac{1}{2}(\hbar\gamma/2)^2$$

the roots are complex, corresponding to the third regime in Figs. 2 and 4.

However, such a regime is not physically acceptable, since the probabilities in (3.6) would oscillate, acquiring values above unity or below zero during finite time intervals. The appearance of such a regime is related to the collapse of the weak coupling approximation employed to extract the non-Markovian master equation (2.2). Indeed, it can be shown that the following relation holds:

$$(\Delta H_{\text{int}})^2 = g^2 \sum_{\alpha\mu} |\lambda_{\alpha\mu}|^2 \tag{4.10}$$

where $(\Delta H_{\text{int}})^2$ is the dispersion of the interaction Hamiltonian with respect to the initial state. When this dispersion exceeds the inelasticity spread $\hbar\gamma$ that yields the width of the Breit–Wigner filter, the assumptions giving rise to the latter [or equivalently, to the representation of the correlation propagator in the memory kernel as a damped exponential on an unitary propagator, i.e., Eq. (2.3)] cease to be valid. Consequently, as the second transition is approached in the space of the roots, one should abandon the description (2.2) of the relaxation dynamics and reformulate the problem giving up the above-mentioned approximation.

5. AN APPROXIMATE DESCRIPTION OF THE POLES

We stress that the evolution of the poles displayed in Fig. 2 is not intrinsic to the set of values selected for this calculation, which correspond to a typical nuclear system. The interaction parameters adequate to those systems lie within the neighborhood of the first transition in the single-pole regime and it is of interest to nuclear physicists to find something out regarding the relation between the Markovian and the non-Markovian

poles. Other choices of the parameters shown at the beginning of this section will provoke smooth changes in the shape of the curves in Fig. 2 and preserve the overall features of the regimes and the connecting transitions. However, in the present case it is especially simple to take advantage of some numerics to perform the integration indicated in Eq. (3.8), dropping the unimportant contributions. On one side, one finds that all fermionic momenta (F, z_α, z_μ, k_s) are rather similar, while the phonon momentum q is about 0.3 fm^{-1} . Another small number is the ratio ε_q/mc_s^2 (about 3%), with $\varepsilon_q = \hbar^2 q^2/2m$. Furthermore, one can consider $\Omega \ll \gamma$, and subsequently, $\Omega/(\gamma - \nu) \ll 1$ if $\nu \ll \gamma$. With these relations in view one finds the approximate expression [cf. Eq. (4.7)]

$$\frac{W_+}{\gamma} \left(\frac{\nu}{\gamma} \right) \approx \omega_\lambda r_{\text{eff}}^2 \frac{\hbar q^2 F^2}{m\gamma^2} \frac{1}{1 - \nu/\gamma} \quad (5.1)$$

from which we obtain the value of the ordinate,

$$W_+(0)/\gamma \approx \omega_\lambda r_{\text{eff}}^2 \hbar q^2 (F^2/m\gamma^2) \quad (5.2)$$

According to (5.1), when the root of Eq. (4.2) occurs at a small $\nu_{<}/\gamma$ value (first regime), we find

$$\nu_{<}/\gamma \approx W_+(0)/[\gamma - W_+(0)] \quad (5.3)$$

We remark here that the Markovian pole is the one appearing when $W_+(0) \ll \gamma$; thus, neglecting $W_+(0)$ in the denominator, we find the expression

$$\nu_M = W_+(0) \quad (5.4)$$

which is the eigenvalue equation of the standard QBM model in the Markovian approximation. Equation (5.3) then yields a relation linking the non-Markovian pole to the Markovian one.

Equation (5.1) describes the transition rate to an excellent approximation in almost the whole interval $0 \leq \nu \leq \gamma$. This fact can be appreciated in Fig. 4, where we have drawn, for each curve in Fig. 2 (full lines), the prediction of (5.1) (dotted lines). It is clear that the approximation is practically an exact description of the low-frequency pole and an exceptionally good approach to the high-frequency one. We can then complete our analysis of the physically admissible regimes 1 and 2 and of the first transition in the light of Eq. (5.1), which we can write

$$W_+(x) = W_+(0)/(1 - x) \quad (5.5)$$

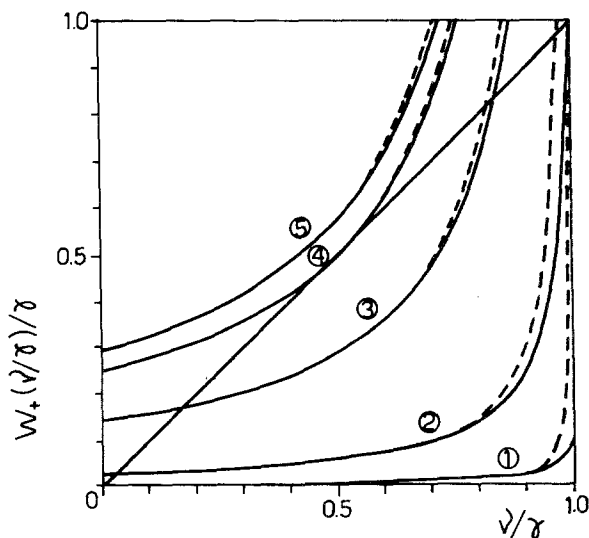


Fig. 4. (—) Same as in Fig. 2; (---) the approximate solution of the pole equation (5.1). The values of the dispersion $(\Delta H_{im})^2$ corresponding to curves 1-5 are, respectively (in MeV^2), 14.44, 144.4, 723.6, 1250.0, and 1444.0.

The pole equation $x = W_+(x)/\gamma$ is a quadratic one in x with solutions [cf. Eq. (4.9)]

$$x = \frac{1}{2} \{ 1 \pm [1 - 4W_+(0)/\gamma]^{1/2} \} \tag{5.6}$$

We see that if $4W_+(0) \ll 1$, a series expansion of (5.6) up to second order for the smallest root leads us once again to (5.3). Recalling now the expression for the amplitude of the time evolution [Eqs. (3.5) and (3.6)], we can write in the single-pole regime

$$\rho_1(t) = \left[\lim_{s \rightarrow s_<} \frac{s - s_<}{s + W_+(s)} \right] e^{s_< t} \tag{5.7}$$

The limit in Eq. (5.7) can be graphically evaluated through either Fig. 2 or Fig. 4, since it can be written

$$\lim_{s \rightarrow s_<} \frac{s - s_<}{s + W_+(s)} = \left[1 - \frac{dW_+(v_<)}{dv} \right]^{-1} \tag{5.8}$$

Using the approximate expression (5.5), we can explicitly calculate the derivative in Eq. (5.8), obtaining

$$\frac{1}{1 - dW_+(v_<)/dv} \approx \frac{\gamma - v_<}{\gamma - 2v_<} \tag{5.9}$$

This directs our attention the fact that for $t=0$ the amplitude is larger than unity. However, one can interpret this as simply bringing into evidence that a macroscopic evolution is only observable for macroscopic times, in our case, for $t \gg \tau_{\text{corr}} = \gamma^{-1}$. Notice that if we look for the time t_0 for which $\rho_1(t_0) = 1$, i.e., for the origin of macroscopic times, it arises from (5.9) that t_0 is precisely the lifetime of correlations γ^{-1} . We ought then to consider expression (5.7) as legitimate for $t > t_0$.

Equation (5.6) cannot describe the first transition, since it takes place outside the range of validity of the approximation (5.5), namely when $x = 1$. However, as the pole $v_>$ decreases, it is rather properly described by the largest root (5.6) (cf. Fig. 4) and the corresponding time evolution can be written as

$$\rho_1(t) = \frac{\gamma - v_<}{\gamma - 2v_<} e^{-v_< t} + \frac{\gamma - v_>}{\gamma - 2v_>} e^{-v_> t} \quad (5.10)$$

Opposite to what happens in the single-pole regime, this evolution law is valid for any time, since, according to (5.6), one can verify that

$$\rho_1(0) = \frac{\gamma - v_<}{\gamma - 2v_<} + \frac{\gamma - v_>}{\gamma - 2v_>} = 1 \quad (5.11)$$

The second transition is contained in Eq. (5.6) and corresponds to the condition $W_+(0)/\gamma = 1/4$. Considering (5.2), we locate the value of the interaction parameter at this point,

$$[\omega_\lambda r_{\text{eff}}^2]_2 = m\gamma^2/4\hbar q^2 F^2 \quad (5.12)$$

and following the geometric interpretation outlined in Section 4 for the first transition, we may consider that the finite duration of the collisions provokes an effective enlarging of the oscillator dispersion in the two-pole regime.

6. SUMMARY

Our work has aimed at finding some insights and criteria through which one could avoid having to find the exact solution of an integrodifferential, non-Markovian dynamical system and approximate the problem by a differential-in-time, Markovian one. We have illustrated in the framework of a model how such a line of analysis might proceed. In particular, we have seen that it is possible, in a situation where the physical magnitudes reproduce the relations occurring in a typical finite system, i.e., a nucleus, to relate the low-frequency poles of the non-Markovian

resolvent to the lowest nonvanishing eigenvalues of the associated Markovian generator of motion. We have carried out a complete discussion and offered possible physical interpretations of the three different regimes that characterize the dynamics under consideration.

APPENDIX

Let us indicate the steps leading from the expression (2.7) for the microscopic transition rates $W_{\pm}(s)$ and the explicit integrals (2.14). We first explicitly introduce the momentum conservation relation $\mathbf{k}_\alpha = \mathbf{k}_\mu + \mathbf{q}$, perform the summation over momenta \mathbf{k}_α , and replace the remaining sum over \mathbf{k}_μ by an integration. In order to write the integrand, we examine the arguments depending on both \mathbf{k}_α and \mathbf{k}_μ and impose momentum conservation, obtaining the following results:

1. Argument of the Breit–Wigner filter:

$$\begin{aligned} \frac{\epsilon_{\alpha\mu}}{\hbar} &= \omega_{\alpha\mu} - \Omega \\ &= \frac{1}{\hbar} \left[\frac{\hbar^2}{2m} (\mathbf{k}_\alpha^2 - \mathbf{k}_\mu^2) - \hbar c_s q \right] \\ &= \frac{\hbar q^2}{2m} + q \left(\frac{\hbar z}{m} - c_s \right) \end{aligned} \tag{A1}$$

with z denoting the z component of momentum \mathbf{k}_μ .

2. Fermi factor in $W_+(s)$:

$$\begin{aligned} F_+(r, z) = \rho_\mu(1 - \rho_\alpha) &= \frac{1}{1 + \exp[(r^2 + z^2 - F^2)/k_T^2]} \\ &\times \frac{1}{1 + \exp\{[-r^2 - (z + q)^2 + F^2]/k_T^2\}} \end{aligned} \tag{A2}$$

with F the Fermi momentum,

$$k_T^2 = 2mT/\hbar^2 \tag{A3}$$

and r the polar component of momentum \mathbf{k}_μ .

3. The Fermi factor in $W_-(s)$,

$$\begin{aligned} F_-(r, z) = \rho_\alpha(1 - \rho_\mu) &= \frac{1}{1 + \exp\{[r^2 + (z + q)^2 - F^2]/k_T^2\}} \\ &\times \frac{1}{1 + \exp[-(r^2 + z^2 - F^2)/k_T^2]} \end{aligned} \tag{A4}$$

Accordingly, we may write

$$\begin{aligned}
 W_{\pm}(s) &= \frac{2g^2}{\hbar^2} \sum_{\alpha\mu} |\lambda_{\alpha\mu}|^2 \delta_{\mathbf{k}_\alpha, \mathbf{k}_\mu + \mathbf{q}} \frac{s + \gamma}{(s + \gamma)^2 + (\varepsilon_{\alpha\mu}/\hbar)^2} \rho_{\alpha}^{\mu} (1 - \rho_{\alpha}^{\mu}) \\
 &= \frac{2g^2}{\hbar^2} |\lambda|^2 \left(\frac{L}{2\pi}\right)^3 2\pi \int_0^{\infty} r dr \int_{-q/2}^{\infty} dz \frac{s + \gamma}{(s + \gamma)^2 + [\varepsilon(z)/\hbar]^2} F_{\pm}(r, z)
 \end{aligned} \tag{A5}$$

We have adopted the criterion $|\lambda_{\alpha\mu}|^2 = |\lambda|^2 \theta(z + q/2)$ in order to ensure that at zero temperature, particle deexcitation due to phonon destruction is not allowed to take place. It becomes clear after inspection of (A2) and (A4) that the radial integrations can be performed analytically,

$$R_{\pm}(z) = 2 \int_0^{\infty} r dr F_{\pm}(r, z) \tag{A6}$$

The results of these integrations are displayed in Eqs. (2.15). It is worthwhile pointing out that the relationship (2.15b) gives

$$W_{-}(s) = e^{-\hbar\Omega/T} W_{+}(s) \tag{A7}$$

if the collisions are energy-conserving, since in the latter case we have, for the argument in the exponential in (2.15b),

$$\frac{\hbar^2}{2mT} [z^2 - (z + q)^2] = -\frac{\hbar^2}{2mT} (2zq + q^2) = -\frac{\hbar c_s q}{T} \tag{A8}$$

the latter equality being a consequence of (A1). In other words, in the case of strict energy conservation at the collision vertex one recovers the canonical or Gibbsian equilibrium solution

$$\rho_n^{(0)}(T) = \frac{1}{Z(T)} \left[\frac{W_{-}(0)}{W_{+}(0)} \right]^n = \frac{1}{Z(T)} e^{-nh\Omega/T} \tag{A9}$$

ACKNOWLEDGMENTS

We are grateful to the Programa de Investigaciones en Física del Plasma at our home institution for access to their computing facilities. This research was supported by grant PID 30529 from Consejo Nacional de Investigaciones Científicas y Técnicas of Argentina.

REFERENCES

1. E. S. Hernández and C. O. Dorso, *Phys. Rev. C* **29**:1510 (1984).
2. C. O. Dorso and E. S. Hernández, *Phys. Rev. C* **29**:1523 (1984).
3. V. de la Mota, C. O. Dorso, and E. S. Hernández, *Phys. Lett. B* **143**:279 (1984).
4. E. S. Hernández and C. O. Dorso, *Phys. Rev. C* **30**:1711 (1984).
5. E. S. Hernández, *Physica* **132A**:28 (1985).
6. E. S. Hernández and A. Kievsky, *Phys. Rev. A* **32**:1810 (1985).
7. H. M. Cataldo, E. S. Hernández, and C. O. Dorso, *Physica* **142A**:498 (1987).
8. A. Kievsky and E. S. Hernández, *Physica* **139A**:149 (1986).
9. E. S. Hernández and A. Kievsky, *Phys. Rev. A* **34**: 2433 (1986).
10. E. S. Hernández and H. M. Cataldo, *Physica* **142A**:517 (1987).
11. A. Kievsky and E. S. Hernández, to be published.
12. A. van der Woude, *Prog. Part. Nucl. Phys.*, to be published.
13. F. Haake, in *Springer Tracts in Modern Physics*, Vol. 66 (Springer, Berlin, 1973).
14. S. Nakajima, *Prog. Theor. Phys.* **20**:948 (1958).
15. R. W. Zwanzig, in *Lectures in Theoretical Physics*, W. S. Brittin, B. W. Downs, and J. Downs, eds. (Interscience, New York, 1961).
16. C. George, I. Prigogine, and L. Rosenfeld, *Mat. Fys. Medd.* **38**:12 (1972).
17. I. Prigogine, C. George, F. Henin, and L. Rosenfeld, *Chem. Scripta* **4**:5 (1972).
18. R. Balescu, *Equilibrium and Nonequilibrium Statistical Mechanics* (Wiley, Interscience, New York, 1975).
19. E. B. Davies, *Commun. Math. Phys.* **39**:91 (1974).
20. H. M. Cataldo and E. S. Hernández, to be published.
21. R. Benguria and M. Kac, *Phys. Rev. Lett.* **46**:1 (1981).
22. H. Maassen, *J. Stat. Phys.* **34**:239 (1984).
23. M. Despósito, Seminar Work, University of Buenos Aires (1986), unpublished.